

The host galaxy of a narrow-line Seyfert 1 galaxy RE J1034+396 with X-ray quasi-periodic oscillations

Wei-Hao Bian^{*} and Kai Huang

Department of Physics and Institute of Theoretical Physics, Nanjing Normal University, Nanjing 210097, China

31 October 2018

ABSTRACT

Using simple stellar population synthesis, we model the bulge stellar contribution in the optical spectrum of a narrow-line Seyfert 1 galaxy RE J1034+396. We find that its bulge stellar velocity dispersion is $67.7 \pm 8 \text{ km s}^{-1}$. The supermassive black hole (SMBH) mass is about $(1 - 4) \times 10^6 M_{\odot}$ if it follows the well-known $M_{\text{BH}} - \sigma_*$ relation found in quiescent galaxies. We also derive the SMBH mass from the $H\beta$ second moment, which is consistent with that from its bulge stellar velocity dispersion. The SMBH mass of $(1 - 4) \times 10^6 M_{\odot}$ implies that the X-ray quasi-periodic oscillation (QPO) of RE J1034+396 can be scaled to a high-frequency QPO at 27-108 Hz found in Galactic black hole binaries with a $10 M_{\odot}$ black hole. With the mass distribution in different age stellar populations, we find that the mean specific star formation rate (SSFR) over past 0.1 Gyr is $0.0163 \pm 0.0011 \text{ Gyr}^{-1}$, the stellar mass in the logarithm is 10.155 ± 0.06 in units of solar mass, and the current star formation rate is $0.23 \pm 0.016 M_{\odot} \text{ yr}^{-1}$. RE J1034+396 does not follow the relation between the Eddington ratio and the SSFR suggested by Chen et al., although a larger scatter in their relation. We also suggest that about 7.0% of the total $H\alpha$ luminosity and 50% of the total [O II] luminosity come from the star formation process.

Key words: galaxies: bulge — galaxies: nuclei — black hole physics — galaxies: stellar content — Galaxy:individual: RE J1034+396

1 INTRODUCTION

It is thought that active galactic nuclei (AGN) are scaled-up versions of Galactic black hole binaries (BHs; Gierlinski et al. 2008 and reference therein). The power spectrum of the X-ray variability in BHs shows the quasi-periodic oscillations of 0.01-450 Hz (QPOs; Rimillard & McClintock 2006). It is believed that we can also find the QPOs in AGN, on the similar behavior of accretion flow around the black hole (BH). Comparing to a BH of $10 M_{\odot}$ in BHs, the typical high-frequency QPOs of 100 Hz would be smaller by 10^6 (i.e., $\sim 10^{-4}$ Hz) for a supermassive black hole (M_{BH} ; SMBH) of $10^7 M_{\odot}$ if the QPO frequencies scale inversely with the BH mass (Rimillard & McClintock 2006).

With a long XMM-Newton observation (91 ks), Gierlinski et al. (2008) detected a significant QPO signal ($\nu = 2.7 \times 10^{-4}$ Hz, corresponding to a period of about 1 hour) for a nearby ($z=0.043$) spiral active galaxy RE J1034+396 (J2000, RA=158.66082, DEC=39.64119). It is optically classified as a narrow-line Seyfert 1 galaxy (NLS1), with similar small line width for the high-ionization and low-ionization

emission lines (Puchnarewicz et al. 1998), and a very soft X-ray spectrum (Grupe et al. 2004; Casebeer et al. 2006). NLS1s are thought to be a special subclass of AGN harboring relatively small but growing SMBHs, compared with other broad-line Seyfert 1 galaxies (BLS1s; e.g. Osterbrock & Pogge 1985; Boller, Brandt & Fink 1996; Mathur 2000). By methods of the standard accretion disk model fitting of spectral energy distribution (SED; Puchnarewicz et al. 2001), the slim disk fitting of SED (Wang et al., 1999; Wang & Netzer 2003), the full width at half-maximum (FWHM) of the $H\beta$ line, [O III] FWHM, and soft X-ray luminosity, the SMBH mass in RE J1034+396 can not be determined very well, from 6.3×10^5 to $3.6 \times 10^7 M_{\odot}$ (Bian et al. 2004; Wang & Lu 2001). Its QPO type (high-frequency or low-frequency QPOs) can not be uniquely identified (Gierlinski et al. 2008).

In the past two decades, there has been striking progress in finding more reliable methods to calculate SMBHs masses in AGN through the line width, ΔV , of $H\beta$ (or $H\alpha$, Mg II , C IV) from the broad line region (BLR) and the BLR size, R_{BLR} (e.g., Kaspi et al. 2000; McLure & Dunlop 2004; Bian & Zhao 2004; Peterson et al. 2004; Greene & Ho 2005b; Bian et al. 2008). There are mainly two ways to parameterize the

^{*} whbian@njnu.edu.cn

line widths of broad emission lines, i.e., FWHM and the second moment (σ_{line}) (e.g. Bian et al. 2008). The second moment of the broad components of the $H\beta$ line provides a more precise measurement of the SMBH mass because the $H\beta$ profile is non-Gaussian in NLS1s. It is suggested that the mean value of the SMBH masses in NLS1s from the $H\beta$ second moment is larger by about 0.50 dex than that from FWHM (Bian et al. 2008). The well-known $M_{BH} - \sigma_*$ relation of inactive galaxies (Tremaine et al. 2002) can also be used to estimate the SMBH mass when the stellar velocity dispersion, σ_* , is available (Kauffmann et al. 2003; Onken et al. 2004; Greene & Ho 2006).

The X-ray QPOs frequency may depend on the mass and the spin of BH (Rimillard & McClintock 2006). The SMBH masses are important in the study of QPOs in AGN. Here we use the Sloan Digital Sky Survey (SDSS; Abazajian et al. 2009) data of this object to determine its SMBH mass by its σ_* and $H\beta$ second moment instead of $H\beta$ FWHM in Bian et al. (2004), as well as the star formation history of its host bulge by the simple stellar population (SSP) synthesis. All of the cosmological calculations in this paper assume $H_0 = 70 \text{ km s}^{-1} \text{ Mpc}^{-1}$, $\Omega_M = 0.3$, and $\Omega_\Lambda = 0.7$.

2 DATA AND ANALYSIS

The SDSS used a dedicated 2.5-m wide-field telescope at Apache Point Observatory near Sacramento Peak in Southern New Mexico to conduct an imaging and spectroscopic survey for about 1/4 sky area. The SDSS data have been made public in a series of yearly data releases and the present is the Seventh Data Release (DR7), including data up to the end of SDSS-II in July, 2008.

The optical spectrum of RE J1034+396 is downloaded from SDSS DR7. Its spectrum covers the wavelength range of 3800-9200 Å with a spectral resolution of $1800 < R < 2100$. At its redshift of 0.043, the projected fiber aperture diameter of 3" is about 2.4 kpc, containing most light from its bulge. With nuclei spectrum superimposed on it, the stellar absorption features in its SDSS spectrum provide us the possibility to investigate the property of its host bulge, including the bulge stellar velocity dispersion, the stellar mass, and the star formation history. We did not apply aperture correction to the stellar velocity dispersion because this effect can be omitted for $z < 0.3$ (Bernardi et al. 2003).

We outline our steps to do the SDSS spectral analysis. (1) We use SSP synthesis (STARLIGHT; Cid Fernandes et al. 2005) to model the stellar contribution in the Galactic extinction-corrected spectrum in the rest frame (Cid Fernandes et al. 2005; Bian et al. 2006, 2007, 2008). The Galactic extinction law of Cardelli, Clayton & Mathis (1989) with $R_V = 3.1$ is adopted, which is also used for the host extinction with V-band extinction (from 0 mag to 5.0 mag). We use 45 default templates in Cid Fernandes et al. (2005), which are calculated from the model of Bruzual & Charlot (2003). The linear combination of 45 templates is used to represent the host bulge spectrum. These 45 templates comprise 15 ages, $t = 0.001, 0.00316, 0.00501, 0.01, 0.02512, 0.04, 0.10152, 0.28612, 0.64054, 0.90479, 1.434, 2.5, 5, 11$ and 13 Gyr, and three metallicities, $Z = 0.2, 1$ and $2.5 Z_\odot$ (Cid Fernandes et al. 2005). At the same time as the SSP

fit, we add a power-law component in the code to represent the AGN continuum emission, and an optical Fe II template from the prototype NLS1 I ZW 1 (Boroson & Green 1992) to model the Fe II emission. We exclude the AGN mission lines, such as H Balmer lines, [O II] $\lambda 3727$, [Ne III] $\lambda 3869$, [O III] $\lambda \lambda 4959, 5007$, [N II] $\lambda \lambda 6548, 6583$, [S II] $\lambda \lambda 6717, 6731$.

The synthetic spectrum is built using the following equation,

$$M_\lambda = M_{\lambda_0} \left[\sum_{j=1}^{N_*} x_j b_{j,\lambda} r_\lambda \otimes G(v_0, v_d) + x_{fe} \otimes G(v_{fe}, \sigma_{fe}) \right] \quad (1)$$

where $b_{j,\lambda}$ is the j^{th} template normalized at $\lambda_0 = 4020 \text{ \AA}$, x_j is the flux fraction at 4020 Å, M_{λ_0} is the synthetic flux at 4020 Å, $r_\lambda \equiv 10^{-0.4(A_\lambda - A_{\lambda_0})}$ is the reddening term by V-band extinction A_V , and $G(v_0, v_d)$ is the line-of-sight stellar velocity distribution, modeled as a Gaussian centered at velocity v_0 and broadened by the velocity dispersion v_d . Due to different velocity dispersion in the stellar lines and Fe II lines, we use another line-of-sight Fe II velocity distribution $G(v_{fe}, \sigma_{fe})$ for the Fe II emission. x_{fe} is the Fe II flux-fraction at 4020 Å. The line-of-sight Fe II velocity distribution $G(v_{fe}, \sigma_{fe})$ is also modeled as a Gaussian centered at velocity v_{fe} and broadened by the velocity dispersion σ_{fe} . We first fit the Fe II lines and the continuum in the fitting windows. And we find that $\sigma_{fe} = 411 \pm 46 \text{ km s}^{-1}$. σ_{fe} is fixed by 411 km/s in the fitting of SSP and Fe II. When we change σ_{fe} , the SSP and Fe II fitting results do not change, considering the errors. We also exclude the Fe II emissions and do the SSP fit, considering the errors, the SSP results do not change. The best fit is reached by minimizing reduced χ^2 ,

$$\chi^2(x, M_{\lambda_0}, A_V, v_0, v_d) = \sum_{\lambda=1}^{N_\lambda} [(O_\lambda - M_\lambda) w_\lambda]^2 / N \quad (2)$$

where the weighted spectrum w_λ is defined as the noise associated with each spectral bin as reported by the SDSS pipeline output, N is the total unmasked pixels. χ^2 is calculated by the difference between observed spectrum and the model spectrum in the fitting of SSP and Fe II. For RE J1034+396, the best fit of SSP and Fe II gives $\chi^2 = 1.4$ (Fig 1). We find that $A_V = 0$, and the host extinction can be neglected (Fig 1). Through above spectral synthesis, we can obtain some parameters, such as bulge velocity dispersion v_d , flux-fraction x_j , mass-fraction μ_j , stellar mass M_* . The mass-flux ratio can be found in STARLIGHT manual on the web site <http://www.starlight.ufsc.br/>. The results are shown in Fig. 1 and Table 1.

With the simulation, it is suggested that the uncertainty of SSP results can be given by the effective starlight signal-to-noise (S/N) at 4020 Å (Cid Fernandes et al. 2005; Bian et al. 2007). The S/N at 4020 Å is 37 and the starlight fraction at 4020 Å is about 43% (Table 1). Therefore the effective starlight S/N at 4020 Å is about 16, corresponding to an uncertainty of 8 km s^{-1} for the velocity dispersion, 7% for the mass-fraction, 8% for the flux-fraction, 0.06 dex for stellar mass $\log M_*$ (Cid Fernandes et al. 2005; Bian et al. 2007). We adopt 10% as the uncertainty of host bulge flux fraction.

(2) Considering the broad wing in the $H\beta$ line profile, two broad components are used to model broad $H\beta$ profile from BLRs. The $H\beta$ line from the narrow line regions

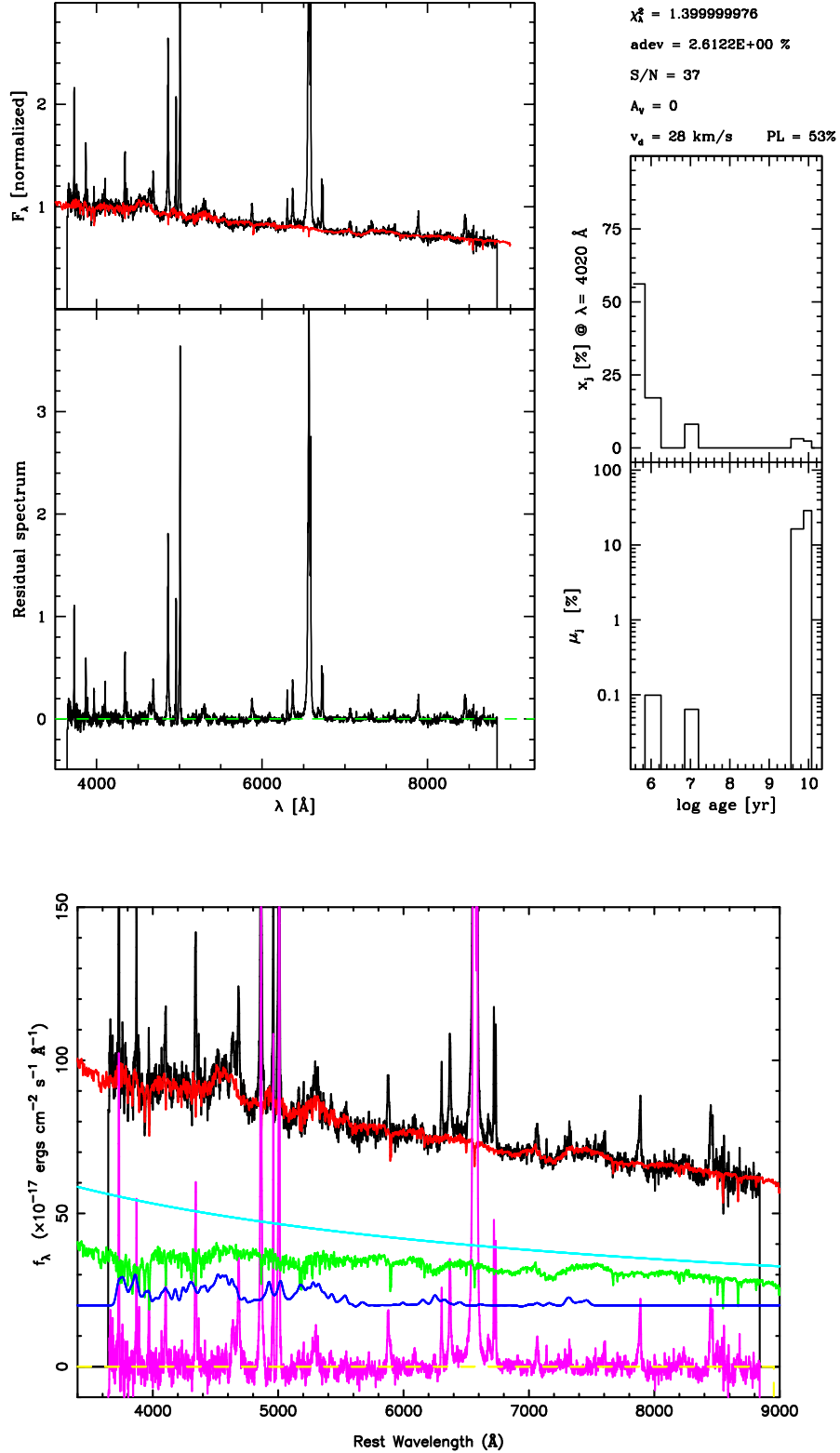


Figure 1. Results of simple stellar population (SSP) synthesis for the SDSS spectrum of RE J1034+396. Top panel: the left panels are the observed and the synthesis spectra (black and red, respectively), and the residual spectrum. The panels on the right show the flux-fraction x_j and mass-fraction μ_j versus the ages of the simple stellar populations. Bottom panel: the black line is the observed SDSS spectrum corrected for Galactic extinction in the rest frame. The cyan line is the power-law continuum. The green line is the host contribution. The blue line is the Fe II spectrum. The magenta line is the residue. The red line is the composition of the host contribution, Fe II lines and the power-law continuum.

Table 1. The host bulge properties of RE J1034+396

| σ_* (km s ⁻¹) (1) | $\log M_*(M_\odot)$ (2) | $SSFR(\text{Gyr}^{-1})$ (3) | f_{host} (4) |
|---|----------------------------|--------------------------------|--------------------------|
| 67.7 ± 8 | 10.155 ± 0.06 | 0.0163 ± 0.0011 | $43 \pm 4\%$ |

Note. Col(1): the host bulge stellar velocity dispersion; Col(2): the stellar mass; Col(3): the host bulge specific star formation rate; Col(4): the host bulge flux fraction at 4020 Å with 10% uncertainty.

Table 2. The emission lines properties of RE J1034+396

| | FWHM ^a | flux ^b |
|-----------------------|-------------------|-------------------|
| H β | 1690 ± 296 | 1.1 ± 0.84 |
| | 617 ± 155 | 0.88 ± 0.73 |
| | 1022 ± 4592^n | 0.10 ± 0.63 |
| | 292 ± 114^n | 0.12 ± 0.13 |
| [O III] | 1023 ± 18^n | 1.26 ± 0.03 |
| | 292 ± 5^n | 1.43 ± 0.03 |
| H α | 969 ± 552 | 3.98 ± 3.15 |
| | 3804 ± 1100 | 2.25 ± 0.39 |
| | 272 ± 25^n | 1.16 ± 0.25 |
| | 1162 ± 275^n | 1.09 ± 2.75 |
| [N II] $\lambda 6583$ | 278 ± 80^n | 1.16 ± 0.08 |
| | 1162 ± 287^n | 1.1 ± 2.81 |
| Fe II | 967 ± 108 | 1.76 ± 0.2^c |

Note. ^a: FWHM of a Gaussian profile in units of km s⁻¹. ^b: in units of 10^{-14} erg s⁻¹ cm⁻². ^c: Fe II flux between 4434 Å and 4684 Å. ⁿ: the components from NLRs. The second weaker broad component of H α is probably due to the contribution from the continuum subtraction.

(NLRs) has the same profile as the [O III] line from NLRs. Two components are used to model the asymmetric [O III] line profile, and two components are used to model H β line profile from NLRs (Bian et al. 2008). Therefore, total four Gaussians are used to model the H β line profile, and two sets of two Gaussians are used to model the [O III] $\lambda\lambda 4959, 5007$ lines. As the same as the H β profile, four Gaussians are used to model the H α profile (two broad components from BLRs and two narrow components from NLRs), and two sets of two Gaussian are used to model the [N II] $\lambda\lambda 6548, 6583$ lines. We take the same line width for each corresponding component of [O III] $\lambda\lambda 4959, 5007$ and H β from NLRs, fix the flux ratio of [O III] $\lambda 4959$ to [O III] $\lambda 5007$ to be 1:3, and set the wavelength separation to the laboratory value. We take the same line width for each corresponding component of [N II] $\lambda\lambda 6548, 6583$ and H α from BLRs, fix the flux ratio of [N II] $\lambda 6548$ to [N II] $\lambda 6583$ to be 1:3, and set the wavelength separation to the laboratory value. For RE J1034+396, the best fits of the H β , H α lines give reduced $\chi^2 = 2.2$, $\chi^2 = 2.14$, respectively. The results are shown in Fig. 2 and Table 2. The third component of the H β line from NLRs is weaker, the results do not change if we remove this weaker component.

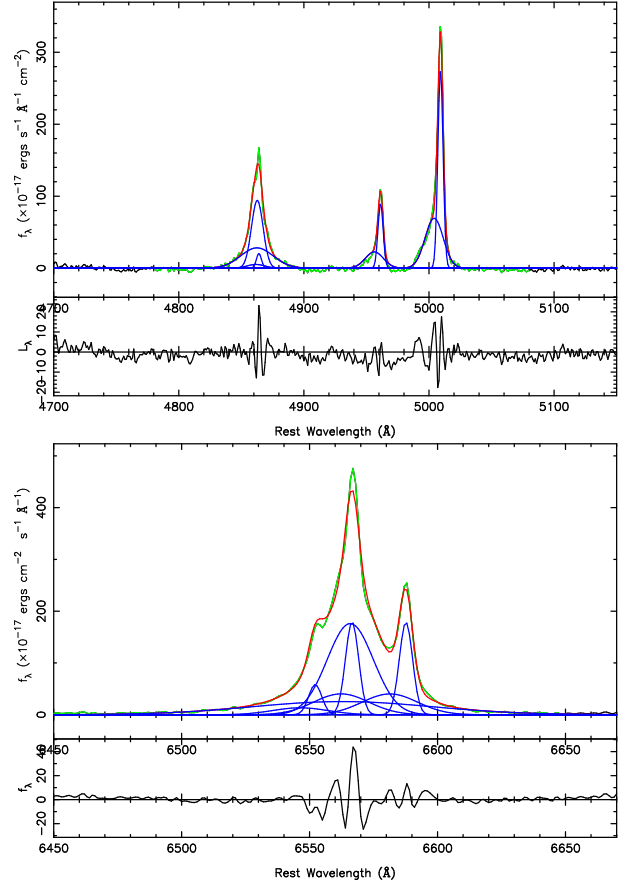


Figure 2. An example of the line fit for RE J1034+396. Top panel: the line fit for H β and [O III] line. The black line is the original spectrum after Galactic-extinction correction, the starlight subtraction, the power-law continuum and the Fe II subtraction in the rest frame. The residual is shown at the bottom. The multiple Gaussian components are in blue and the sum of them is in red. The fitting window is in green. Bottom panel: the line fit for H α and [N II] line. The line colors are the same to that in top panel.

3 RESULT AND DISCUSSION

3.1 Mass

Firstly, we derive the mass from the bulge stellar velocity dispersion, σ_* . By SSP method, the measured bulge stellar velocity dispersion v_d is 28 ± 8 km s⁻¹. Considering the resolutions of the SDSS spectra and the template spectra, we have to do these corrections by the following formula ¹,

$$\sigma_* = \sqrt{v_d^2 + \sigma_{\text{temp}}^2 - \sigma_{\text{inst}}^2} \quad (3)$$

where the SDSS spectral resolution σ_{inst} is adopted as 60 km s⁻¹ (Greene & Ho 2005a), the template spectral resolution σ_{temp} is adopted as 86 km s⁻¹ (Cid Fernandes et al. 2005). Assuming that the errors on σ_{inst} and σ_{temp} are negligible, the error on σ_* will be the same as that on v_d . $v_d = 28 \pm 8$ km s⁻¹ leads to $\sigma_* = 67.7 \pm 8$ km s⁻¹. Using the $M_{\text{BH}} - \sigma_*$ relation for quiescent galaxies, $M_{\text{BH}}(\sigma_*) = 10^{8.13} [\sigma_*/(200 \text{ km s}^{-1})]^{4.02} M_\odot$ (Tremaine et al. 2002), we

¹ <http://www.starlight.ufsc.br/>

derive the SMBH mass is $(1.7^{+1.0}_{-0.7}) \times 10^6 M_\odot$ for $\sigma_* = 67.7 \pm 8 \text{ km s}^{-1}$. The uncertainty of 8 km s^{-1} for σ_* would lead to an error of 0.1 dex for $\log M_{\text{BH}}$. The total uncertainty is about 0.32 dex considering the error of 0.3 dex from the $M_{\text{BH}} - \sigma_*$ relation (Tremaine et al. 2002). Therefore, the SMBH mass of RE J1034+396 derived from σ_* is about $(1 - 4) \times 10^6 M_\odot$.

Secondly, we derive the mass from the broad H β second moment $\sigma_{\text{H}\beta}$ and the empirical $R_{\text{BLR}} - \lambda L_\lambda(5100\text{\AA})$ relation (Kaspi et al. 2000, 2005; Bentz et al. 2006; Bian et al. 2008). With the power-law component, we can derive the nuclear flux at 5100 \AA is $45 \times 10^{-17} \text{ erg s}^{-1} \text{ cm}^{-2}$, and $\lambda L_\lambda(5100\text{\AA})$ is $5.6 \times 10^{42} \text{ erg s}^{-1}$. The first moment of the line profile $P(\lambda)$ is

$$\lambda_0 = \frac{\int \lambda P(\lambda) d\lambda}{\int P(\lambda) d\lambda}, \quad (4)$$

The second moment of the line profile $P(\lambda)$ is

$$\sigma_{\text{line}}^2 = \frac{\int \lambda^2 P(\lambda) d\lambda}{\int P(\lambda) d\lambda} - \lambda_0^2. \quad (5)$$

For a Gaussian line profile, the ratio of FWHM to the second momentum is $\text{FWHM}/\sigma_{\text{line}} = \sqrt{8\ln 2} \approx 2.35$; while for a Lorentzian profile, $\sigma_{\text{line}} \rightarrow \infty$. For RE J1034+396, the H β second momentum $\sigma_{\text{H}\beta}$ is calculated from the reconstructed H β profile of two broad H β components from BLRs in step 2 of spectral analysis, and $\sigma_{\text{H}\beta}$ is $577 \pm 144 \text{ km s}^{-1}$. From the reconstructed H β profile from BLRs, FWHM is $802 \pm 200 \text{ km s}^{-1}$. The SMBH mass can be calculated from the H β second moment by the following equation (Bian et al. 2008),

$$M_{\text{BH}} = f \frac{R_{\text{BLR}} \Delta V^2}{G} \\ = f \times 7.629 \times 10^6 \left[\frac{\lambda L_\lambda(5100\text{\AA})}{10^{44} \text{ erg s}^{-1}} \right]^{0.518} \left[\frac{\sigma_{\text{H}\beta}}{1000 \text{ km s}^{-1}} \right]^2 M_\odot \quad (6)$$

where $R_{\text{BLR}} = 39.08 \times [\lambda L_\lambda(5100\text{\AA}) / (10^{44} \text{ erg s}^{-1})]^{0.518}$ light-days (Bentz et al. 2006), and $f = 3.85$ (Collin et al. 2006). With $\sigma_{\text{H}\beta} = 577 \pm 144 \text{ km s}^{-1}$ and $f = 3.85$, the estimated SMBH mass is $(0.7 - 3.4) \times 10^6 M_\odot$. The uncertainty of the mass calculation from the H β line is mainly from the systematic uncertainties, up to about 0.5 dex, which is due to the unknown kinematics and geometry in BLRs (e.g. Krolik 2001; Peterson et al. 2004). Grupe et al. (2004) gave $\lambda L_\lambda(5100\text{\AA})$ as $1.5 \times 10^{43} \text{ erg s}^{-1}$. Considering the half light contribution from the host bulge, the nuclear $\lambda L_\lambda(5100\text{\AA})$ is consistent with ours. They also gave the H β FWHM as $700 \pm 110 \text{ km s}^{-1}$. When using this FWHM value to calculate the mass, the mass would be smaller by 0.5 dex than that from the $\sigma_{\text{H}\beta}$ (Bian et al. 2004, 2008). The new mass from the H β second moment is consistent with that from the $M_{\text{BH}} - \sigma_*$ relation. Hereafter, we adopt $(1 - 4) \times 10^6 M_\odot$ as its SMBH mass. This SMBH mass value of RE J1034+396 is consistent with that derived from the accretion disk fitting of its SED (Puchnarewicz et al., 2001; Wang & Netzer 2003).

It is suggested that the gaseous kinematics of NLRs be primarily governed by the bulge gravitational potential. Using the linewidth of [O III] or [N II] to trace the σ_* , we find that, from narrow [O III] component, $\sigma_{[\text{O III}]}$ = 124 km s^{-1} (see Table 2). It would lead to a mass of $2 \times 10^7 M_\odot$, which is larger than mass from σ_* and $\sigma_{\text{H}\beta}$ by an order of

magnitude. For RE J1034+396, $\sigma_{[\text{O III}]}$ cannot be used to trace σ_* .

3.2 High-frequency QPOs and BH spin

QPOs can be classified as low-frequency QPOs (roughly 0.1-30 Hz) and high-frequency QPOs (roughly 40-450 Hz, Rimillard & McClintock 2006). Assuming QPO frequency (ν_{BHB}) scales inversely with the BH mass (M_{BHB}) in BHBs, $M_{\text{BH}}/M_{\text{BHB}} = \nu_{\text{BHB}}/\nu_{\text{BH}}$, where ν_{BH} is the QPO frequency for SMBH in AGN. By $\nu_{\text{BHB}} = \nu_{\text{BH}} \times (M_{\text{BH}}/M_{\text{BHB}})$, the QPO frequency of $2.7 \times 10^{-4} \text{ Hz}$ in RE J1034+396 (its SMBH mass of $2 \times 10^6 M_\odot$ with an uncertain of a factor 2) corresponds a frequency of 27-108 Hz in Galactic BHBs with a $10 M_\odot$ BH. Our result of 27-108 Hz suggests that the QPO found in RE J1034+396 belongs to a high-frequency QPO. Larger estimated SMBH mass, smaller adopted BHBs mass would make this frequency value larger.

It is believed that the high-frequency QPOs may depend only on the mass and the spin of the BH. This dependence can be expected for coordinate frequencies (see Merloni et al. 1999) or for disk oscillation modes in the inner accretion disk (see Kato 2001). For a Schwarzschild BH, the innermost stable circular orbit (ISCO) corresponds a maximum orbit frequency as $\nu_{\text{ISCO}} = 2200(M_{\text{BH}}/M_\odot)^{-1} \text{ Hz}$. For an extreme Kerr BH, $\nu_{\text{ISCO}} = 16150(M_{\text{BH}}/M_\odot)^{-1} \text{ Hz}$ (Rimillard & McClintock 2006). For three BHBs with high-frequency QPOs and well-constrained BH masses, Rimillard & McClintock (2006) suggested an empirical frequency - mass relation for the high-frequency QPOs, $\nu_0 = 931(M_{\text{BH}}/M_\odot)^{-1} \text{ Hz}$. With the SMBH mass of $2 \times 10^6 M_\odot$ in RE J1034+396, the corresponding frequencies derived from the ISCO of a Schwarzschild BH, the ISCO of an extreme Kerr BH, and the empirical frequency - mass relation are 11.0×10^{-4} , 8.0×10^{-4} , $4.7 \times 10^{-4} \text{ Hz}$, respectively. Considering an uncertainty of a factor of 2 in the SMBH mass and other uncertainty in empirical frequency - mass relation for the high-frequency QPOs (e.g., the BH spin), the double or triple value of the fundamental frequency $4.7 \times 10^{-4} \text{ Hz}$ dose not deviate much from the observed frequency of $2.7 \times 10^{-4} \text{ Hz}$ in RE J1034+396. It implies that the QPOs phenomenon has the same origin in BHBs and AGN (e.g., Gierlinski 2008).

3.3 Star formation

The widely employed method to measure the current star formation rates (SFR) is by means of the ultraviolet continuum, the emission lines of H α , [O II], et al. (Kennicutt 1998). For a sample of 82302 star formation galaxies from SDSS, Asari et al. (2007) investigated the current SFR derived from the SSPs synthesis and found that it is consistent with that from the H α SFR indicator (see their Fig. 6). The current specific SFR (SSFR) is defined by the mean SSFR over the past 0.1 Gyr, i.e., first 21 of the 45 templates described in section 2 with age less than 0.1 Gyr (Asari et al. 2007; Chen et al. 2009),

$$\text{SSFR}(t < 0.1 \text{ Gyr}) = \frac{\text{SFR}}{M_*} = \frac{\sum_{j=1}^{21} \mu_j}{0.1 \text{ Gyr}} \quad (7)$$

For RE J1034+396, current SSFR($t < 0.1 \text{ Gyr}$) is $0.0163 \pm 0.0011 \text{ Gyr}^{-1}$, $\log M_*$ is $10.155 \pm 0.06 M_\odot$, and current SFR

is $0.23 \pm 0.016 M_{\odot} \text{yr}^{-1}$. Using the SFR formula from Kennicutt et al. (1998), this current SFR of $0.23 \pm 0.016 M_{\odot} \text{yr}^{-1}$ corresponds to the $\text{H}\alpha$ luminosity as $(2.9 \pm 0.2) \times 10^{40} \text{ erg s}^{-1}$ or the $[\text{O II}]$ luminosity as $(1.6 \pm 0.1) \times 10^{40} \text{ erg s}^{-1}$ coming from the starburst process. From the SDSS spectrum, we find that total $\text{H}\alpha$ luminosity and total $[\text{O II}]$ luminosity is $4.4 \times 10^{41} \text{ erg s}^{-1}$, $3.4 \times 10^{40} \text{ erg s}^{-1}$. Therefore, about 6.1%-7.0% of the total $\text{H}\alpha$ luminosity and 44%-50% of the total $[\text{O II}]$ luminosity come from the star formation (Ho 2005).

We also use 150 templates instead of 45 templates in SSP synthesis to model the stellar absorption contribution, like in Asari et al. (2007). We found that $\sigma_* = 72.4 \text{ km s}^{-1}$, $\log M_* = 10.244$, $\text{SSFR}(t < 0.1 \text{ Gyr}) = 0.02786 \text{ Gyr}^{-1}$. Using 150 templates, the σ_* and $\log M_*$ are consistent with that using 45 templates, the stellar flux fraction is 47%, and the SSFR would be larger by 70%.

Using type-II AGN sample from MPA/JHU catalog (Kauffmann et al. 2003), Chen et al. (2009) found a correlation between the Eddington ratio λ (the ratio of the bolometric luminosity, L_{bol} , to the Eddington luminosity, L_{Edd}) and the mean SSFR, $\log \lambda = (-0.73 \pm 0.01) + (1.5 \pm 0.01) \log(\text{SSFR}/\text{Gyr}^{-1})$, suggesting that supernova explosions play a role in the transportation of gas to galactic centers. Considering that the difference between type II AGN and type I AGN is due to the orientation of the line of sight, type I AGN would also follow this $\log \lambda - \log \text{SSFR}$ relation. Here we calculate the Eddington ratio for RE J1034+396. Using $L_{\text{bol}} = 9 \times \lambda L_{\lambda}(5100\text{\AA})$ (Kaspi et al. 2000), $L_{\text{Edd}} = 1.26 \times 10^{38} (M_{\text{bh}}/M_{\odot}) \text{ erg s}^{-1}$, and $M_{\text{BH}} = 2 \times 10^6 M_{\odot}$, we find that the Eddington ratio is 0.2. Considering the uncertainty of a factor of 2 in M_{BH} , the uncertainty of the Eddington ratio is a factor of 2, i.e., $\log \lambda = -1 \sim -0.4$. Using the formula of (3) in Chen et al. (2009), the SSFR of $0.0163 \pm 0.001 \text{ Gyr}^{-1}$ leads to $\log \lambda$ as $-3.45 \sim -3.37$, which deviates much from the value of $-1 \sim -0.4$. The deviation of $\log \lambda$ is $2.37 \sim 3.05$ in the $\log \lambda - \log \text{SSFR}$ diagram of Chen et al. (2009). Considering most of the bolometric luminosity is emitted in the UV and soft X-ray band, Grupe et al. (2004) estimated the bolometric luminosity from a combined power-law model fit with exponential cutoff to the optical-UV data and a power law to the soft X-ray data. They found $L_{\text{bol}} \approx 22 \times \lambda L_{\lambda}(5100\text{\AA})$, which is consistent with its hot big blue bump. If that is the case, $\log \lambda$ would be larger by 0.39. Therefore, RE J1034+396 does not follow the relation between the Eddington ratio and SSFR found by Chen et al. (2009), although a large scatter in their relation. The reason for the deviation would be explored in other place.

4 CONCLUSIONS

The host bulge of a NLS1 RE J1034+396 with X-ray quasi-periodic oscillations is investigated through its optical spectrum from SDSS DR7. The main conclusions can be summarized as follows: (1) The host bulge flux contribution at 4020 \AA is about $(43 \pm 4)\%$ in the SDSS spectrum and the bulge stellar velocity dispersion σ_* is $67.7 \pm 8 \text{ km s}^{-1}$. Considering the scatter in $M_{\text{BH}} - \sigma_*$ relation, the SMBH mass from $M_{\text{BH}} - \sigma_*$ relation is $(1 - 4) \times 10^6 M_{\odot}$. (2) Using multi-Gaussians to model the $\text{H}\beta$, $[\text{O III}]$, $\text{H}\alpha$, and $[\text{N II}]$ emission lines, we find that the mass from $\sigma_{\text{H}\beta}$ and

$\lambda L_{\lambda}(5100\text{\AA})$ is $(0.7 \pm 3.4) \times 10^6 M_{\odot}$, consistent with that from σ_* . However, the $[\text{O III}]$ velocity dispersion is $124 \pm 2 \text{ km s}^{-1}$, about a double of σ_* . (3) The SMBH mass of about $(1 - 4) \times 10^6 M_{\odot}$ implies that the QPO of $2.7 \times 10^{-4} Hz$ found in RE J1034+396 can be scaled to a high-frequency QPO at about 27-108 Hz found in Galactic BHs with a $10 M_{\odot}$ BH. (4) From the SSPs synthesis, we find that current $\text{SSFR}(t < 0.1 \text{ Gyr})$ is $0.0163 \pm 0.0011 \text{ Gyr}^{-1}$, $\log(M_*/M_{\odot})$ is 10.155 ± 0.06 , and current SFR is $0.23 \pm 0.016 M_{\odot} \text{yr}^{-1}$. RE J1034+396 does not follow the relation between the Eddington ratio and SSFR. About 6.1%-7.0% of the total $\text{H}\alpha$ luminosity and 44%-50% of the total $[\text{O II}]$ luminosity come from the star formation process.

ACKNOWLEDGMENTS

This work has been supported by the NSFC (Nos. 10873010 and 1073301) and National Basic Research Program of China - the 973 Program (Grant No. 2009CB824800). We are very grateful to the anonymous referee for her/his constructive comments which significantly improved the content of the paper. We thank J. M. wang, S.N. Zhang, C. Hu, and Q. S., Gu for their useful discussions.

REFERENCES

- Abazajian, K. N., et al., 2009, ApJS, 182,543
 Asari, N. V., et al., 2007, MNRAS, 381,263
 Bentz, M. C., et al., 2006, ApJ, 644, 133
 Bernardi, M., et al., 2003, AJ, 125, 1817
 Bian, W., Zhao, Y., 2004, MNRAS, 352, 823
 Bian, W., et al., 2006, MNRAS, 372, 876
 Bian, W., Chen, Y., Gu Q., Wang, J., 2007, ApJ, 668, 721
 Bian, W., et al., 2008, MNRAS, 390, 752
 Boller, Th., Brandt, W. N., Fink, H., 1996, A&A, 305, 53
 Boroson, T. A., & Green, R. F., 1992, ApJS, 80, 109
 Bruzual, G., Charlot, S. 2003, MNRAS, 344, 1000
 Cardelli, J. A., Clayton, G. C., Mathis, J. S. 1989, ApJ, 345, 245
 Casebeer, D. A., Leighly, K. M., Baron, E., 2006, ApJ, 637, 157
 Chen, Y., et al., 2009, ApJ, 695, L130
 Cid Fernandes, R., Mateus, A., Sodre L., Stasinska, G., Gomes J., 2005, MNRAS, 358, 363
 Collin, S. et al., 2006, A&A, 456, 75
 Gierlinski et al., 2008, Nature, 455, 369
 Greene J. E., Ho L. C., 2005a, ApJ, 627, 721
 Greene, J. E., Ho, L. C., 2005b, ApJ, 630, 122
 Greene, J. E., Ho, L. C., 2006, ApJ, 641, L21
 Grupe, D., et al., 2004, AJ, 127, 156
 Ho, L. C., 2005, ApJ, 629, 680
 Kaspi, S., Maoz, D., Netzer, H., Peterson, B.M., Vestergaard M., Jannuzi B.T., 2005, ApJ, 629, 61
 Kaspi, S., Smith, P.S., Netzer, H., Maoz, D., Jannuzi, B.T., Giveon U., 2000, ApJ, 533, 631
 Kato, S., 2001, PASJ, 53, 1
 Kauffmann, G., et al., 2003, MNRAS, 346, 1055
 Kennicutt, R. C., 1998, ARA&A, 36, 189
 Krolik, J. H., 2001, ApJ, 551, 72
 Mathur, S., Kuraszkiwicz, J., Czerny, B., 2001, NewA, 6, 321
 Merloni, A., Vietri, M., Stella, L, Bini, D., 1999, MNRAS, 304, 155
 McLure, R. J., & Jarvis, M. J., 2004, MNRAS, 353, L45
 Onken, C. A., et al., 2004, ApJ, 615, 645
 Osterbrock, D., & Pogge, R. W., 1985, ApJ, 297, 116
 Peterson, B. M., ApJ, 2004, 613, 682

- Puchnarewicz, E. M., et al., 1998, MNRAS, 293, L52
Puchnarewicz, E. M., Mason, K. O., Siemiginowska, A., et al.
2001, ApJ, 550, 644
Rimillard, R., A., & McClintock, J., E., 2006, ARA&A, 44, 49
Tremaine, S., et al., 2002, ApJ, 574, 740
Wang, J. M., Netzer, H., 2003, A&A, 398, 927
Wang, J. M., Szuszkiewicz, E., Lu, F. J., & Zhou, Y. Y. 1999,
ApJ, 522, 839
Wang, T. G., Lu, Y. J., 2001, A&A, 377,52